Coherent coupling of metamaterial resonators with dipole transitions of boron acceptors in Si

Meng, F.; Han, F.; Kentsch, U.; Pashkin, O.; Fowley, C.; Rebohle, L.; Thomson, M. D.; Suzuki, S.; Asada, M.; Roskos, H. G.;

Originally published:

September 2022

Optics Letters 47(2022), 4969-4972

DOI: https://doi.org/10.1364/OL.466392

Electromagnetic coupling of split-ring resonators with dipole transitions of boron acceptors in Si at 7.33 and 8.28 THz

FANQI MENG[1,5], FEIFAN HAN[2], ULRICH KENTSCH[3], ALEXEJ PASHKIN[3], CIARAN FOWLEY[3], LARS REBOHLE[3], MARK D. THOMSON[1], SAFUMI SUZUKI[2], MASAHIRO ASADA[4], AND HARTMUT G. ROSKOS[1,6]

[1]*Physikalisches Institut, Johann Wolfgang Goethe-Universität, Frankfurt am Main, Germany*
[2]*Department of Electrical and Electronic Engineering, Tokyo Institute of Technology, Tokyo, Japan*
[3]*Institute of Ion Beam Physics and Materials Research, Helmholtz-Zentrum Dresden-Rossendorf, 01328 Dresden, Germany*
[4]*Institute of Innovative Research, Tokyo Institute of Technology, Tokyo, Japan*
[5]*fmeng@physik.uni-frankfurt.de*
[6]*roskos@physik.uni-frankfurt.de*

Abstract: We investigate the coherent coupling of split-ring resonators of a metamaterial with hydrogen-like boron acceptors in Si at cryogenic temperatures. When the resonance frequency of the metamaterial, chosen to be in the range 7-9 THz, superimposes the transition frequency from the ground state of the acceptor to an excited state, Rabi splitting is observed. The splitting shows a square-root dependence on the density of the acceptors. Our experiments may help to open a possible route for the investigation of quantum information processes employing strong coupling of dopants in cavities.

In the past decades, light-matter interaction in photonic cavities has provided a unique testbed for the investigation of fundamental quantum physics. By coupling with the cavity photons, electronic transitions of the material can be substantially modified, especially in the *strong coupling* regime, where polariton quasi-particles are formed [1]. These new dressed states reveal themselves by Rabi-split transitions in the absorption spectra, if the rate of energy exchange between matter and the cavity photons is larger than the rate of energy loss of both cavity and matter. Strong light-matter interaction was first studied with free atoms, and Rabi splitting was reported to be at hundreds of MHz. In recent years, there is an intense interest to explore the *ultra-strong coupling* regime, where the Rabi splitting reaches a substantial portion of the resonance frequency of the cavity [2], and even the *deep strong coupling* regime where the Rabi splitting is larger than the resonance frequency of the cavity [3]. A strong motivation comes from quantum computing and quantum information processing, where coupling of the relevant excitations in cavities plays an important role [4].

Access to these regimes with free atoms is, however, hindered by the relatively weak electron transition dipole moments encountered there [5]. Atoms embedded in a crystalline solid-state matrix are more suitable for such investigations. This is especially true for atoms which represent dilute shallow dopants. Such dopants are essential ingredients of all semiconductor devices. Their energy states can be modeled in a hydrogen-like fashion. Due to the dielectric environment and the orbital interaction with the host material, the transition dipole moments can be several orders of magnitude larger than those of free atoms [6]. At room temperature, the atoms are ionized, and the electrons, respectively holes, are free to move. At low temperature, the charge carriers are frozen in their ground states. Upon irradiation with electromagnetic radiation, the charge carriers can be excited to higher energy states via dipole-allowed transitions. This is one reason

why dopants exhibit great potential for applications in atomic-scale solid-state spintronics [7] and quantum computing [8, 9]. In addition, quantum devices based on dopants in Si can be readily integrated into the current semiconductor technology. In this report, we demonstrate strong interaction of transitions between boron acceptor states in Si with the fundamental-mode plasmonic excitation of split-ring oscillators, observing a Rabi splitting as large as 0.4 THz.

The experiments were performed with boron-doped Si samples prepared by ion implantation of high-resistivity Si wafers (purchased from UniversityWafer Inc., with the thickness of 500 μm). To create a homogenously doped surface layer of 1-μm thickness, multi-energy implantation was employed. Two specimens were prepared with boron densities of 4×10^{16} cm^{-3} and 2×10^{17} cm^{-3}. After implantation, rapid thermal annealing was carried out to remove defects in the Si lattice generated by the implantation [10]. Fig. 1a shows the linear transmission spectrum of an annealed sample with a boron density of 2×10^{17} cm^{-3}, measured by Fourier transform far-infrared spectroscopy at a sample temperature of 20 K (a reference transmission spectrum taken at 100 K was used for background subtraction). The spectrum exhibits the expected series of discrete transitions from the boron ground-state to excited states at 7.33 THz ($1\Gamma_8^+ \rightarrow 1\Gamma_8^-$), 8.28 THz ($1\Gamma_8^+ \rightarrow 2\Gamma_8^-$), 9.5 THz ($1\Gamma_8^+ \rightarrow 1\Gamma_7^-, 1\Gamma_6^-$), and 10.27 THz ($1\Gamma_8^+ \rightarrow 2\Gamma_6^-, 6\Gamma_8^-$) [11]. The transition lines are well separated from each other even at this fairly high dopant density. The widths of the lower two transition lines are 0.18 THz and 0.19 THz, respectively.

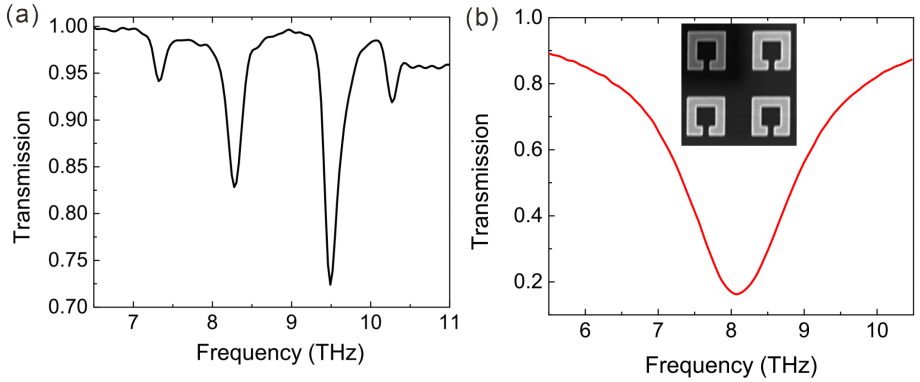

Fig. 1. (a) Measured transmission spectrum of boron-implanted Si at 20 K (boron density: 2×10^{17} cm^{-3}). (b) Measured transmission spectrum of a metamaterial on boron-implanted Si at 100 K. Both figures cover an x-axis range of 5 THz. The inset shows an image taken by atomic force microscopy (AFM) of the gold pattern.

Metamaterial patterns with unit cells consisting of metallic square-shaped split-ring resonators (SRR) were prepared by e-beam lithography on the surfaces of the implanted Si specimens. We designed metamaterials [12] with six different fundamental resonance frequencies to cover the lower two impurity transition lines. An AFM image of four unit cells of one of the fabricated metamaterials is shown in the inset of Fig. 1b. All six metamaterials have the same period, metal stripe width and gap width of 5.2 μm, 0.6 μm and 0.6 μm, respectively. Only the length of the outer edges varies, with values of 3.0, 2.9, 2.8, 2.7, 2.6 and 2.5 μm, respectively. Transmission spectra of the metamaterial-covered doped specimens, which were recorded at a sample temperature of 100 K, where the dopants are ionized and the impurity transitions are absent, revealed frequencies of the fundamental resonances between 7.0 THz and 9.09 THz. A representative spectrum of a metamaterial with a SRR edge length of 2.7 μm is shown in Fig. 1b (the spectrum was derived by subtracting a reference transmission spectrum of an equally doped Si specimen without metamaterial pattern on it). The full width at half maximum of the metamaterial resonance is 1.4 THz, with a Q-factor of 6. The measured resonance frequency is

8.08 THz at 100 K, and decreases to below 8.0 THz at 20 K. Simulations with the CST Maxwell solver, assuming the room-temperature values of the Au conductivity of 4.5×10^6 S/m and of the Si dielectric constant of 11.9, yield a resonance frequency of 8.3 THz [11].

Figure 2a shows transmission spectra of all six metamaterial-covered Si samples with a boron density of 2×10^{17} cm^{-3} at a temperature of 20 K. The positions of the boron acceptor transitions at 7.33 THz, 8.28 THz and 9.5 THz are indicated by vertical dashed lines. The SRR resonances are well below the highest-lying of these three transitions. One finds in the spectra of Fig. 2a, that the frequency of this 9.5-THz transition is not affected by the presence of the metamaterial. In contrast, the two lower transitions (at 7.33 THz and 8.28 THz) exhibit level splitting, if the resonance frequency of the metamaterial is close to the respective acceptor transition line.

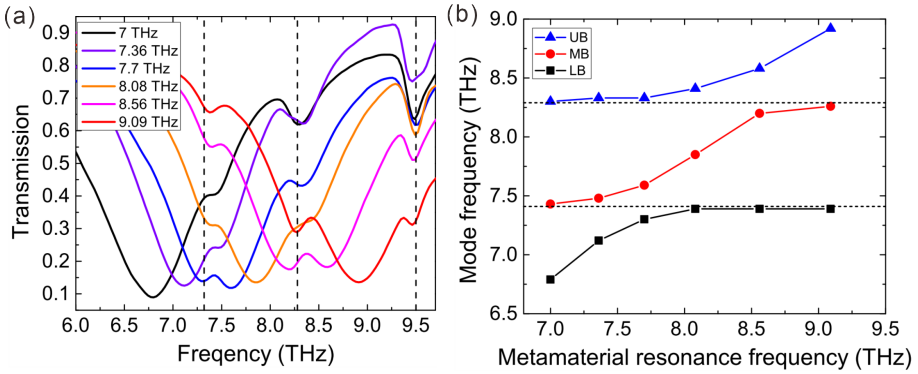

Fig. 2. (a) Transmission spectra of metamaterial-covered doped Si with a boron density of 2×10^{17} cm^{-3} at 20 K. Different colors represent metamaterials of different resonance frequencies. The legend specifies the resonance frequency of the metamaterials measured at 100 K. The vertical dashed lines indicate transition frequencies of the bare dopants. (b) Frequency positions of the transmission minima as a function of the metamaterial's resonance frequency. An avoided-crossing behavior is observed around center frequencies of 7.40 THz and 8.29 THz (marked by dashed horizontal lines), slightly higher than the respective transition frequencies of 7.33 THz and 8.28 THz of the bare impurities.

Figure 2b displays the transmission minima extracted from the spectra as a function of the resonance frequency of the metamaterial. The data points group in three features (branches) which are characteristic for Rabi-split hybrid transitions, as one expects them to arise from the electromagnetic coupling of the metamaterial resonators and the dopants [13]. The three branches are plotted in different coloring: a lower branch (LB, black), a middle branch (MB, red) and an upper branch (UB, blue). They exhibit anti-crossing signatures around frequencies of 7.40 THz and 8.29 THz (marked by horizontal dashed lines in Fig. 2b), slightly higher than the frequencies of the bare impurity transitions. The minimal frequency splitting (Rabi splitting) is 0.3 THz at the lower transition line, and 0.4 THz, respectively, at the higher one. The smaller value of the Rabi splitting at the lower transition line is attributed to a smaller transition dipole moment.

The coupling strength g of light-matter interaction is given by half the Rabi splitting of the ensuing polariton branches. For the second transition, the value of g is hence 0.2 THz. This value is to be compared with the linewidth γ of the bare impurity transition (γ = 0.19 THz). If one assume the linewidth to be of homogeneous nature, it represents the population decay rate of the upper state of the impurity transition. The linewidth of the metamaterial resonance, on the other hand, represents the decay rate of the resonator mode. Fig. 1b yields κ = 1.4 THz. With these values, one finds that the condition $2g < (\gamma + \kappa)/2$ is fulfilled, which implies that the coupled system is not in the strong-interaction regime. Using the classification scheme of

Ref. [14], the relationships $g \approx \gamma$ and $g < \kappa$ categorize the coupled system to be at the boundary between the weak-coupling regime and the electromagnetically induced transparency regime.

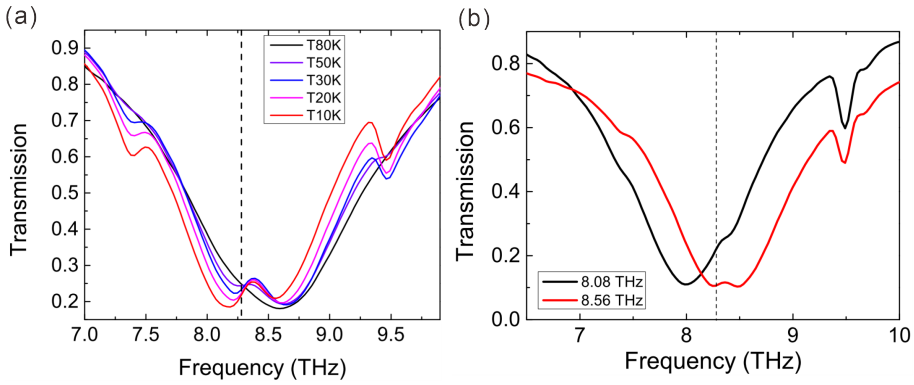

Fig. 3. (a) Temperature dependence of the transmission spectra of Si doped at a boron density of 2×10^{17} cm^{-3} and covered by a metamaterial with a room-temperature SRR resonance at 8.56 THz. Different colors represent different temperatures, as specified in the legend. (b) 20-K transmission spectra of metamaterial-covered doped Si with a boron density of 4×10^{16} cm^{-3}, for two SRR resonances with 100-K resonance positions as indicated in the legend.
The vertical dashed respectively dotted lines indicate the 8.28-THz transition frequency of the bare dopants.

Figure 3a shows the transmission spectra of metamaterial-covered doped Si with a boron density of 2×10^{17} cm^{-3} at different temperatures from 80 down to 10 K. At a temperature of 80 K, the spectra exhibit only the resonance of the metamaterial with a transmission minimum at around 8.56 THz. As the temperature decreases, the absorption features of the boron dopants emerge: The transition lines at 7.33 THz and 9.5 THz, and a double-dip feature around the 8.28-THz transition, indicating Rabi splitting of that transition. As the resonance frequency of the metamaterial shifts to lower frequency when the temperature is decreased further and further, first the high-frequency dip is more pronounced, then it is the low-frequency one. At 20 K, they are almost equally strong, indicating that the resonance frequency of the metamaterial should be close to 8.28 THz at this temperature. The Rabi splitting amounts to 0.4 THz, as discussed previously.

Figure 3b displays two transmission spectra measured with samples with a dopant density of 4×10^{16} cm^{-3} at 20 K. Two different metamaterials are deposited onto the specimens, with resonance frequencies at 8.08 and 8.56 THz (frequencies determined at 100 K). For the metamaterial with a 100-K resonance at 8.08 THz, the resonance frequency of the cavity is detuned from the transition lines, while the resonance curve of the other metamaterial superimposes with the transition line at 8.28 THz. The transmission spectrum measured with that specimen exhibits a Rabi splitting of 0.23 THz at 20 K. Comparing this value with that of the corresponding sample with the higher doping density, one finds that the ratio of the Rabi splittings (0.4/0.22=1.8) is similar to the square root of the doping densities ($\sqrt{2 \times 10^{17}/4 \times 10^{16}} = 2.2$). This is reasonably consistent with the prediction of cavity quantum electrodynamics that the coupling strength should be proportional to the square root of the number of particles involved in the coupling [12]. The difference between these two ratios may be attributed to the uncertainty of the doping density resulting from variations of the ion beam fluences of the multi-energy ion implantation process.

In conclusion, we have achieved coherent interaction between electronic transitions of boron acceptors in Si and metamaterial resonators. A Rabi splitting as large as 0.4 THz is observed. However, due to the low Q-factor of the split-ring resonators of the metamaterial, the coupling

strength is still much less than the dissipation rate of the metamaterial. In order to achieve stronger coupling, a metamaterial with a higher Q-factor, such as toroidal metamaterial [15] or a Fano-type metamaterial [16], should be adopted in the future. Another potential approach is to employ a two-dimensional photonic crystal cavity which possesses a very high Q-factor (of about 1000 [17]), such that it may even be possible to operate in the strong coupling regime while keeping the dopant density low.

Acknowledgements

This research work was funded by DFG project RO 770/41-1 and RO 770/46-1. The authors thank Lichuan Zheng and Sebastian Kölsch for the AFM pictures of the metamaterials.

Disclosures

The authors declare that there are no conflicts of interest related to this article.

Data Availability

Data underlying the results presented in this paper are not publicly available at this time but may be obtained from the authors upon reasonable request.

References

1. S. Haroche, "Nobel lecture: controlling photons in a box and exploring the quantum to classical boundary," Rev. Mod. Phys. **85**, 1083–1102 (2013).
2. G. Scalari, C. Maissen, D. Turcinková, D. Hagenmüller, S. D. Liberato, C. Ciuti, C. Reichl, D. Schuh, W. Wegscheider, M. Beck, and J. Faist, "Ultrastrong coupling of the cyclotron transition of a 2D electron gas to a THz metamaterial," Science **335**, 1323–1326 (2012).
3. A. Bayer, M. Pozimski, S. Schambeck, D. Schuh, R. Huber, D. Bougeard, and C. Lange, "Terahertz light-matter interaction beyond unity coupling strength," Nano Lett. **17**, 6340–6344 (2017).
4. J. M. Gambetta, J. M. Chow, and M. Steffen, "Building logical qubits in a superconducting quantum computing system," npj Quantum Inf. **3** (2017).
5. D. J. Alton, N. P. Stern, T. Aoki, H. Lee, E. Ostby, K. J. Vahala, and H. J. Kimble, "Strong interactions of single atoms and photons near a dielectric boundary," Nat. Phys. **7**, 159–165 (2010).
6. M. A. W. van Loon, N. Stavrias, N. H. Le, K. L. Litvinenko, P. T. Greenland, C. R. Pidgeon, K. Saeedi, B. Redlich, G. Aeppli, and B. N. Murdin, "Giant multiphoton absorption for THz resonances in silicon hydrogenic donors," Nat. Photonics **12**, 179–184 (2018).
7. M. J. Gullans and J. M. Taylor, "Optical control of donor spin qubits in silicon," Phys. Rev. B **92** (2015).
8. P. T. Greenland, S. A. Lynch, , A. F. G. van der Meer, B. N. Murdin, C. R. Pidgeon, B. Redlich, N. Q. Vinh, and G. Aeppli, "Coherent control of Rydberg states in silicon," Nature **465**, 1057–1062 (2010).
9. B. E. Kane, "A silicon-based nuclear spin quantum computer," Nature **393**, 133–137 (1998).
10. J. Narayan and O. W. Holland, "Rapid thermal annealing of ion-implanted semiconductors," J. Appl. Phys. **56**, 2913–2921 (1984).
11. F. Meng, M. D. Thomson, Q. ul Islam, B. Klug, A. Pashkin, H. Schneider, and H. G. Roskos, "Intracavity third-harmonic generation in Si:B pumped by intense terahertz pulses," Phys. Rev. B **102**, 075205 (2020).
12. F. Meng, M. D. Thomson, B. Klug, D. Čibiraitė, Q. ul Islam, and H. G. Roskos, "Nonlocal collective ultrastrong interaction of plasmonic metamaterials and photons in a terahertz photonic crystal cavity," Opt. Express **27**, 24455–24468 (2019).
13. F. Meng, M. D. Thomson, B. Klug, and H. G. Roskos, "Strong interaction between two photons and a plasmon of a complementary metamaterial in a terahertz dual cavity," Opt. Express **29**, 42420 (2021).
14. X. Zhang, C. L. Zou, L. Jiang, and H. X. Tang, "Strongly coupled magnons and cavity microwave photons," Phys. Rev. Lett. **113**, 156401 (2014).
15. T. Kaelberer, V. A. Fedotov, N. Papasimakis, D. P. Tsai, and N. I. Zheludev, "Toroidal dipolar response in a metamaterial," Science **330**, 1510–1512 (2010).
16. V. A. Fedotov, M. Rose, S. L. Prosvirnin, N. Papasimakis, and N. I. Zheludev, "Sharp trapped-mode resonances in planar metamaterials with a broken structural symmetry," Phys. Rev. Lett. **99** (2007).
17. C. M. Yee and M. S. Sherwin, "High-Q terahertz microcavities in silicon photonic crystal slabs," Appl. Phys. Lett. **94**, 154104 (2009).